Comparison of Backscattering Models at L-Band for Growing Corn

Alejandro Monsivais-Huertero, *Member, IEEE*, and Jasmeet Judge, *Senior Member, IEEE*

***Abstract*—The impact of incoherent and coherent formulations on estimates of terrain backscatter ($\sigma^0_{\text{terrain}}$) at L-band for a growing season of corn is examined. The average root mean square difference (RMSD) between the two formulations over the growing season ranged between 3–4 dB, with higher RMSDs at HH polarization (pol), indicating the presence of coherent effects. In the incoherent model, the direct scattering from stems was the primary mechanism, while in the coherent formulation, the interactions between the stems and soil were the primary mechanisms due to the coherent effects. Both incoherent and coherent formulations estimated equally high sensitivities of $\sigma^0_{\text{terrain}}$ to soil moisture (SM) during early stage under low vegetation conditions. During the early and mid stages, the $\sigma^0_{\text{terrain}}$ estimated by both formulations exhibited higher sensitivities during dry conditions than wet conditions. In contrast, during the reproductive stage, the $\sigma^0_{\text{terrain}}$ by the incoherent formulation was more sensitive to the SM at wet conditions than at dry conditions. Based upon the ALOS/SMAP accuracy for $\sigma^0_{\text{terrain}}$, the incoherent formulation exhibited the highest sensitivity during the early stage with detection of SM changes as low as 2 vol% for dry condition, whereas the coherent formulation exhibited the highest sensitivity during the mid stage with detection of SM changes as low as 2.5 vol%. The results of this study suggest that the coherent effects should be considered for defining accuracy of SM estimation algorithms for corn at L-band.**

***Index Terms*—Backscatter for dynamic vegetation, coherent and incoherent scattering models, soil moisture (SM), soil moisture sensitivity.**

I. Introduction

SOIL moisture (SM) is an important land surface variable for understanding the following: 1) water cycle; 2) ecosystem productivity; and 3) linkages between water, energy, and carbon cycles. Low microwave frequencies, particularly at < 10 GHz, are highly sensitive to moisture in the upper few centimeters of the soil. For SM studies, observations at L-band frequencies of 1.2–1.4 GHz are more desirable than higher frequencies due to the larger penetration depths. Currently, there are two operational satellite-based microwave sensors at L-band: 1) the ALOS/PALSAR [1]; and 2) the European Space Agency's Soil Moisture and Ocean Salinity (SMOS) mission [2]. The NASA/CONAE Aquarius [3] and NASA Soil Moisture Active/Passive (SMAP) [4] missions are planned for launch in the near future. The SMAP mission will include active and passive sensors at L-band to provide global observations of SM, with a repeat coverage of every 2–3 days [4]. Both the active (radar) and passive (radiometer) microwave sensors measure radiation quantities that are functions of the soil dielectric constant and exhibit similar sensitivities to SM. In addition to the SM sensitivity, radar backscatter is highly sensitive to the roughness of the soil surface and scattering within the vegetation. These effects may produce a much larger dynamic range in backscatter than that produced due to the SM changes alone. While significant progress has been made in developing and validating forward models for passive studies, a gap still remains in such activities for active studies particularly under dynamic vegetation conditions [5]. These forward models are essential for effective assimilation and SM retrieval algorithms with active and passive observations, such as those from the SMAP mission.

The goal of this study is to understand the impact of the differences in the implementation of biophysics and soil–vegetation interactions in various backscattering algorithms on the overall backscatter under dynamic vegetation conditions, such as growing corn. This understanding is critical for improving backscattering algorithms for both assimilation and retrieval studies. Very few studies have been conducted at L-band for dynamic vegetation [6], when scattering within the vegetation and interactions between vegetation and soil increase. The objectives of this study are the following: 1) to compare two backscattering models for a growing season of sweet corn in Florida; and 2) investigate the sensitivity of overall backscatter in these models to changes in SM during the growing season to assess the potential use of the active observations during the different growth stages. In this study, we use the incoherent Michigan Microwave Canopy Scattering (MIMICS) model [7], and the coherent model with random (CoR) [8] vegetation generator. The soil and vegetation characteristics in the models were obtained from the field observations during the Fifth Microwave Water and Energy Balance Experiment (MicroWEX-5) [9].

II. Scattering From Vegetated Terrain

The backscatter from a vegetated terrain ($\sigma^0_{\text{terrain}}$) is given as

$$\sigma^0_{\text{terrain}} = \sigma^0_{\text{soil}} + \sigma^0_{\text{dir}} + \sigma^0_{\text{int}} \tag{1a}$$

$$\sigma^0_{\text{terrain}} = \sigma^0_{\text{soil}} + \sigma^0_{\text{l,dir}} + \sigma^0_{\text{se,dir}} + \sigma^0_{\text{l,int}} + \sigma^0_{\text{se,int}} \tag{1b}$$

where σ^0_{soil} and σ^0_{dir} represent the direct backscatter from soil and vegetation, respectively, and σ^0_{int} represents the interactions between vegetation and soil. The $\sigma^0_{\text{l,dir}}$ and $\sigma^0_{\text{l,int}}$ are the direct

Manuscript received October 9, 2009; revised February 23, 2010 and April 19, 2010; accepted April 23, 2010. Date of publication June 21, 2010; date of current version December 27, 2010. This work was supported by the NASA-Terrestrial Hydrology Program (THP)-NNX09AK29G. Partial support for MicroWEX-5 was obtained from the National Science Foundation's Earth Science Division (EAR-0337277) and the NASA New Investigator Program (NASA-NIP-00050655).

The authors are with the Center for Remote Sensing, Agricultural and Biological Engineering Department, Institute of Food and Agricultural Sciences, University of Florida, Gainesville, FL 32611 USA (e-mail: monsivais@ufl.edu).

Digital Object Identifier 10.1109/LGRS.2010.2050459

TABLE I
GROWTH STAGES OF SWEET CORN DURING THE MICROWEX-5 FROM [15]

Stage	DoY	Height (cm)	LAI	Characteristics
Early	68-95	< 33	< 0.2	Almost bare soil; emergence DoY 72
Mid	95-115	33 – 167	0.2 – 2.5	Maximum vegetative growth; tasseling on DoY 109
Reproductive	115-150	167 – 186	2.5 – 2.8	Silking on DoY 115; ear formation on DoY 116

scattering from leaves and from the interactions between leaves and soil, respectively. The $\sigma^0_{\rm se,dir}$ and $\sigma^0_{\rm se,int}$ are the direct scattering from stems and from the interactions between stems and soil, respectively.

The $\sigma^0_{\rm soil}$ is a function of soil reflectivity and is typically estimated using surface scattering models such as the following: 1) Small Perturbation Method (SPM); 2) the Kirchhoff Approximation (KA) or 3) the Integral Equation Method (IEM) [10]. The $\sigma^0_{\rm dir}$ is a function of the canopy opacity and geometry. The $\sigma^0_{\rm int}$ is a function of SM, canopy opacity, and geometry. Both the $\sigma^0_{\rm dir}$ and $\sigma^0_{\rm int}$ are usually estimated using either Radiative Transfer (RT)/incoherent, Coherent (CO), or Canopy Semi-Empirical (CSE) formulations. The RT and the CO formulations are based upon the interactions of the electromagnetic wave with discretized vegetation, whereas the CSE models are based upon the regression analyses of the radar backscatter observations or simulations. In the incoherent formulation, the RT equation balances the amplitudes of the incoming and outgoing energies across an elemental volume [7]. In contrast, the coherent approaches calculate both the amplitude and phase of a scattered field by constituent elements of a vegetation, such as the following: 1) branches; 2) stems; 3) leaves, etc.

III. MicroWEX-5

The MicroWEX-5 experiment was conducted during a growing season of sweet corn in North Central Florida from Day of Year (DoY) 68 (March 9) to DoY 150 (May 30) in 2006 [9]. The experimental site was 37 000 $\rm m^2$, where the soil was composed of 89.4% by vol. fine sand and 7.1% by vol. clay. The corn was planted at a row spacing of 76 cm, with a stand density of 8 plants/$\rm m^2$. During the MicroWEX-5, observations were conducted for micrometeorological, soil, and vegetation conditions throughout the growing season. 68 observations of soil profiles were obtained to compute the roughness parameters using a 2-m-long mesh board, following the procedure described in [11]. Weekly observations of vegetation conditions such as the following: 1) the height; 2) vertical distribution of moisture; 3) biomass; and 4) LAI were obtained. Table I shows the three growth stages of corn and their associated vegetation characteristics observed during the MicroWEX-5. Geometrical description of vegetation components such as stems, leaves, and ears were derived from weeky digital pictures. SM values were observed every 15 min at 0–5 cm.

IV. METHODOLOGY

In this study, we estimate $\sigma^0_{\rm soil}$ for bare soil at 1.26 GHz with an incidence angle of 40° using the IEM with an exponential correlation function. The SPM and KA were not applicable because roughness values of $h_{\rm rms} = 1.4$ cm; $l_c = 4.65$ cm, measured at the MicroWEX-5 site [11] where beyond their

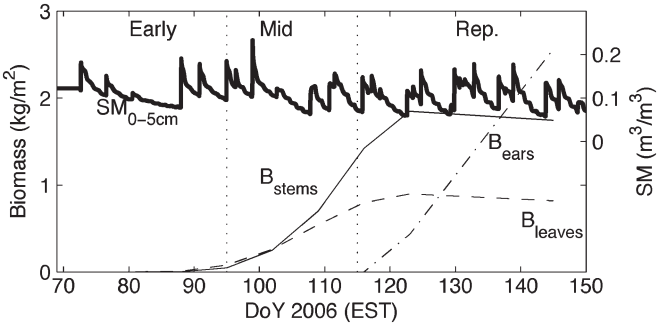

Fig. 1. Soil moisture (SM) at 0–5 cm and biomass for stems, leaves, and ears observed during the MicroWEX-5.

TABLE II
VEGETATION PARAMETERS USED IN THIS STUDY. ALL THE PARAMETERS WERE OBSERVED DURING MICROWEX-5

	Parameters	Values	Models
Canopy	Height (m)	0 - 1.9	MIMICS, CoR
Stems	Length (m)	0 - 1.3	MIMICS, CoR
	Radius (cm)	0 - 0.9	MIMICS, CoR
	Moist. content ($\frac{kgm^{-2}}{kgm^{-2}}$)	0.1 - 0.6	MIMICS, CoR
	Density (# /m^2)	8	MIMICS, CoR
	Euler angle α (deg)	0 - 360	MIMICS, CoR
	Euler angle β (deg)	0 - 5	MIMICS, CoR
Leaves	Thickness (m)	0.35	MIMICS, CoR
	Moist. content ($\frac{kgm^{-2}}{kgm^{-2}}$)	0.09 - 0.94	MIMICS, CoR
	Radius (cm)	0 - 13.0	MIMICS
	Major-axis (cm)	0 - 52.0	CoR
	Minor-axis (cm)	0 - 4.7	CoR
	Density (# /m^3)	72.7 - 393.0	MIMICS, CoR
	Euler angle α (deg)	0 - 360	MIMICS, CoR
	Euler angle β (deg)	0 - 15	MIMICS, CoR
Ears	Length (m)	0 - 0.2	MIMICS, CoR
	Radius (cm)	0 - 2.9	MIMICS, CoR
	Moist. content ($\frac{kgm^{-2}}{kgm^{-2}}$)	0 - 0.4	MIMICS, CoR
	Density (# /m^2)	8	MIMICS, CoR
	Euler angle α (deg)	0 - 360	MIMICS, CoR
	Euler angle β (deg)	0 - 55	MIMICS, CoR

ranges of validity. The SM values at 0–5 cm observed during the MicroWEX-5 (Fig. 1) were used to estimate the soil permittivities using Peplinski *et al.* [12]. The vegetation permittivities were estimated using Ulaby and El-Rayes [13].

We estimate the $\sigma^0_{\rm terrain}$ at VV ($\sigma^0_{\rm terrainVV}$) and HH ($\sigma^0_{\rm terrainHH}$) polarizations (pols) during the growing season of sweet corn, from DoY 68-150, during the MicroWEX-5 using MIMICS [7] and CoR [8] models. The $\sigma^0_{\rm terrain}$ was estimated at 1.26 GHz and 40° incidence angle. Both the models, developed for forest, were adapted to corn. The trunk layer was replaced by a single-layered corn vegetation, with one class of cylindrical stems and one class of leaves. The stems were modeled as discs during the early stage when the stem height and the stem diameter were similar and as thin cylinders as the crop height increased. The leaves were modeled as discs (MIMICS) and ellipsoids (CoR) and the ears were modeled as stems. The distribution of the scatterers inside the vegetation, representing the tree crown in the original models, was changed to a uniform distribution. Parameters related to stems, leaves, and ears for this study were obtained from MicroWEX-5 and are given in Table II. For the CoR model, the average $\sigma^0_{\rm terrain}$ was estimated using the Monte Carlo method with 400 realizations to ensure an oscillation amplitude in the $\sigma^0_{\rm terrain} < 0.25$ dB.

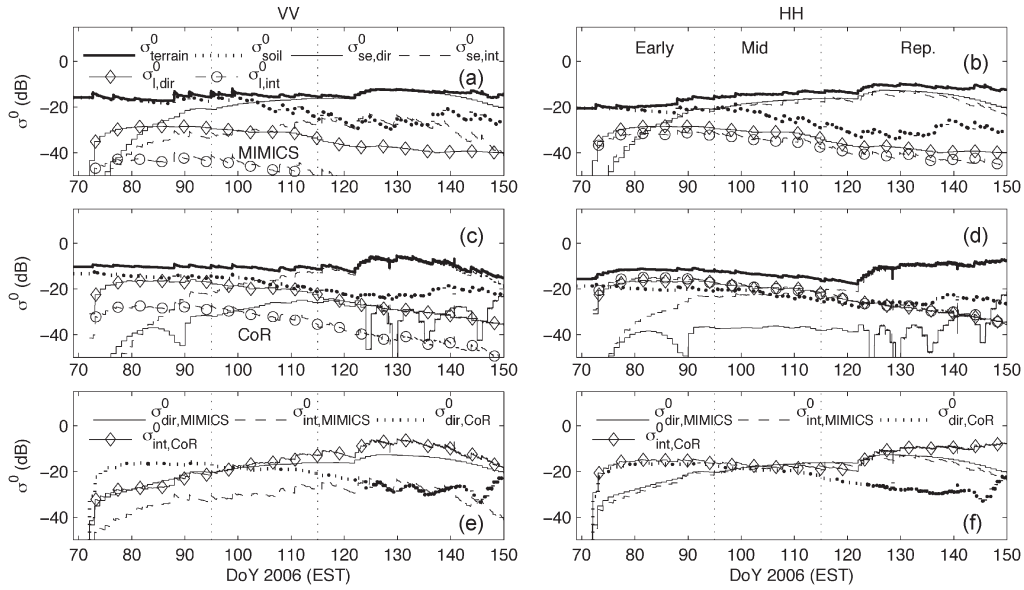

Fig. 2. $\sigma^0_{\rm terrain}$ and contributions of each term in (1) estimated for the growing season during MicroWEX-5 by (a) the MIMICS model at VV pol, (b) at HH pol, (c) the CoR model at VV pol, (d) at HH pol, (e) the $\sigma^0_{\rm dir}$ and $\sigma^0_{\rm int}$ estimated by the MIMICS and CoR models at VV pol, and (f) at HH pol.

V. Results and Discussion

A. $\sigma^0_{\rm terrain}$ for Growing Season of Corn

1) Growing Season: Fig. 2 compares the $\sigma^0_{\rm terrainVV}$ and $\sigma^0_{\rm terrainHH}$ obtained by the MIMICS and CoR models. The MIMICS model estimated a lower dynamic range of $\sigma^0_{\rm terrainVV}$ (5 dB), indicating lower sensitivity to dynamic vegetation compared to the 10-dB range estimated by the CoR model. The ranges estimated by both the models were similar for $\sigma^0_{\rm terrainHH}$ of 8–9 dB. The average root mean square difference (RMSD) between the two models during the growing season ranged between 3–4 dB, with higher RMSDs at HH pol, similar to those in [6], due to coherent effects. The lowest RMSDs of 3.2 dB at VV and 1 dB at HH between the models were observed during the mid stage, when the vegetation height increased from 33 to 167 cm, and the largest RMSD of 4.2 dB at VV and 2.2 dB at HH were observed during the reproductive stage, coinciding with the growing of ears (see Figs. 1 and 2). Fig. 2(a)–(f) show the contribution of each term in (1) by the two models and Table III gives the relative contribution of the terms toward the total $\sigma^0_{\rm terrain}$. In both the incoherent (MIMICS) and the coherent (CoR) models, the contribution from leaves, $\sigma^0_{\rm l,dir}+\sigma^0_{\rm l,int}$, dominated during the early stage, whereas the contribution from stems, $\sigma^0_{\rm se,dir}+\sigma^0_{\rm se,int}$, dominated from early mid stage to the end of the season [Fig. 2(a)–(d)]. As expected, $\sigma^0_{\rm se,dir}$ was the primary contribution in the incoherent model [Fig. 2(a) and (b)], whereas $\sigma^0_{\rm se,int}$ was the most siginificant in the coherent model [Fig. 2(c) and (d)] due to the constructive interferences of backscattered and incident waves transmitting through the same inhomogeneities with the vegetation [8]. The incoherent models calculate only amplitudes and do not consider such interferences. Both the coherent and incoherent models predicted a difference of about 10 dB between $\sigma^0_{\rm l,dir}$ and $\sigma^0_{\rm l,int}$ at VV pol [Fig. 2(a) and (c)], whereas predicted similar amplitudes at HH pol [Fig. 2(b) and (d)]. The $\sigma^0_{\rm se,dir}$ and $\sigma^0_{\rm se,int}$ were similar at HH pol in the MIMICS model, whereas the CoR model predicted a difference of 14 dB at VV and 17 dB at HH during the season, suggesting that HH pol is more sensitive to the coherent effects of the stem. The disc-shaped leaves in MIMICS predicted lower $\sigma^0_{\rm l,dir}$ and $\sigma^0_{\rm l,int}$ at both pols than those predicted by the ellipsoidal leaves, that are geometrically better representatives for corn leaves, in the CoR model. Inclusion of ellipsoidal leaves in MIMICS may result in an increase of 5–10 dB in the $\sigma^0_{\rm l,dir}$ and $\sigma^0_{\rm l,int}$ [compare Fig. 2(a) and (b) to (c) and (d)].

TABLE III
Relative Contributions of Soil ($R_{\rm s}=\sigma^0_{\rm soil}/\sigma^0_{\rm terrain}$), Vegetation ($R_{\rm v}=\sigma^0_{\rm dir}/\sigma^0_{\rm terrain}$), Soil–Vegetation Interactions ($R_{\rm sv}=\sigma^0_{\rm int}/\sigma^0_{\rm terrain}$) and the Sensitivity of $\sigma^0_{\rm terrain}$ to Changes in SM ($m=\Delta\sigma^0_{\rm terrain}/\Delta$SM) for Dry and Wet Conditions

Pol.	Model		Season	Early	Mid	Reprod.
VV	MIMICS	R_s (%)	42	89	42	12
		R_v (%)	53	10	54	81
		R_{sv} (%)	5	1	4	7
		m_{dry} (dB/vol%)	0.23	0.45	0.18	0.09
		m_{wet} (dB/vol%)	0.21	0.34	0.18	0.13
	CoR	R_s (%)	22	40	25	6
		R_v (%)	33	57	40	8
		R_{sv} (%)	45	3	35	86
		m_{dry} (dB/vol%)	0.20	0.20	0.31	0.15
		m_{wet} (dB/vol%)	0.15	0.17	0.19	0.13
HH	MIMICS	R_s (%)	25	68	15	2
		R_v (%)	18	40	47	53
		R_{sv} (%)	14	35	38	45
		m_{dry} (dB/vol%)	0.26	0.24	0.32	0.29
		m_{wet} (dB/vol%)	0.28	0.17	0.21	0.54
	CoR	R_s (%)	12	21	15	3
		R_v (%)	30	46	43	4
		R_{sv} (%)	58	33	42	93
		m_{dry} (dB/vol%)	0.23	0.20	0.25	0.21
		m_{wet} (dB/vol%)	0.21	0.17	0.18	0.34

2) Early Stage: During the early stage, the MIMICS model predicts higher values of $\sigma^0_{\rm terrainVV}$ than those of $\sigma^0_{\rm terrainHH}$, while CoR model predicted similar values at both co-pols [see Fig. 2(a)–(d)]. The $\sigma^0_{\rm terrainVV}$ by the two models MIMICS and CoR and the $\sigma^0_{\rm terrainHH}$ by the CoR model showed similar trend as SM variations [compare Fig. 1 to Fig. 2(a)–(c)]. The $\sigma^0_{\rm soil}$ in MIMICS was the largest of the $\sigma^0_{\rm terrain}$ in the early

stage [Fig. 2(a) and (b)]. In contrast, the $\sigma^0_{\rm dir}$ and $\sigma^0_{\rm int}$ were unrealistically larger than the $\sigma^0_{\rm soil}$ contribution in the CoR model [see Fig. 2(e) and (f)] because of the high contribution from the leaves ($\sigma^0_{\rm l,dir}$ and $\sigma^0_{\rm l,int}$), even when the vegetation cover was minimal [compare Fig. 2(c) with (d)]. Because of the small dimensions of leaves, the sizes estimated for the ellipsoids were unrealistically large at this stage. More accurate estimates of leaf sizes were obtained during MicroWEX-5 once the leaves grew larger.

3) Mid Stage: During the mid stage, the $\sigma^0_{\rm terrainVV}$ estimated by both the MIMICS and CoR models ranged between -18 and -6 dB and $\sigma^0_{\rm terrainHH}$ ranged between -18 and -10 dB, similar to [5]. In the CoR model, the stem contribution increased significantly at both co-pols, compared to the increase in the leaf contribution due to higher increase in the stem biomass [see Figs. 1 and 2(c) and (d)]. At VV pol, the $\sigma^0_{\rm dir}$ and $\sigma^0_{\rm int}$ estimated by the MIMICS model continued to increase due to vegetation growth [Fig. 2(e)]. The $\sigma^0_{\rm soil}$ of -15 dB, was the primary contribution in the early mid stage DoY 95–104, when the vegetation increased from 6–167 cm [Fig. 2(a) and (b)]. In contrast, the $\sigma^0_{\rm dir}$ decreased in the CoR model, while the $\sigma^0_{\rm int}$ increased significantly [Fig. 2(e)]. The $\sigma^0_{\rm dir}$ had the highest contribution during DoY 95–100, primarily from leaves ($\sigma^0_{\rm l,dir}$) and $\sigma^0_{\rm int}$ had the highest contribution after DoY 100, primarily from stems $\sigma^0_{\rm se,int}$) [see Fig. 2(c) and (e)]. At the HH pol, both the $\sigma^0_{\rm dir}$ and $\sigma^0_{\rm int}$ in the MIMICS model increased and had similar values. Both $\sigma^0_{\rm se,dir}$ and $\sigma^0_{\rm se,int}$ had the highest contributions for the entire mid stage, indicating stem as the primary contribution [Fig. 2(b)]. The $\sigma^0_{\rm dir}$ decreased throughout the mid stage, and the $\sigma^0_{\rm int}$ decreased up to DoY 104 and increased during the late mid stage (DoY 104–115) [Fig. 2(f)]. The $\sigma^0_{\rm dir}$ and $\sigma^0_{\rm int}$ estimated by the CoR model had equally high contributions up to DoY 104 and $\sigma^0_{\rm int}$ during the late mid stage, DoY 104–115 [see Fig. 2(f)].

4) Reproductive Stage: During the reproductive stage, both the MIMICS and CoR models estimated maximum $\sigma^0_{\rm terrain}$ values in the growing season at both co-pols [see Fig. 2(a)–(d)]. The MIMICS model predicted similiar magnitudes of $\sigma^0_{\rm terrainVV}$ and $\sigma^0_{\rm terrainHH}$ [see Fig. 2(a) and (b)], while the $\sigma^0_{\rm terrainVV}$ predicted by CoR model was lower than the $\sigma^0_{\rm terrainHH}$, particularly, at the end of the season [see Fig. 2(c) and (d)]. In the MIMICS model, the $\sigma^0_{\rm dir}$ had the highest contribution at VV [Fig. 2(e)], while both $\sigma^0_{\rm dir}$ and $\sigma^0_{\rm int}$ had similar magnitudes at HH pol [Fig. 2(f)]. In the CoR model, $\sigma^0_{\rm int}$ had the highest contribution at both co-pols [Fig. 2(e) and (f)]. Although the leaf biomass remained almost constant after DoY 122, the two models showed a decrease in the leaf contribution [see Figs. 1 and 2(a)–(d)] primarily due to the increased extinction from the developing ear. The CoR model predicted values of $\sigma^0_{\rm se,int}$ and $\sigma^0_{\rm se,dir}$ with oscillations > 0.4 dB after DoY 130, when the ear biomass > 0.5 [see Figs. 1 and 2(c) and (d)]. Even though the ear formation occurred on DoY 116, their effects on $\sigma^0_{\rm se,int}$ and $\sigma^0_{\rm se,dir}$ were not observed until DoY 125 and 130, respectively, when the ear length was about 2 cm. The oscillations of $\sigma^0_{\rm se,int}$ and $\sigma^0_{\rm se,dir}$ could be because the ears were distributed randomly between 0–1.8 m, for each realization of the CoR model. The ears were located between 30–50 cm above the soil surface during MicroWEX-5. Constraining the ear location in the CoR model could result in convergence of $\sigma^0_{\rm se,dir}$ and $\sigma^0_{\rm se,int}$.

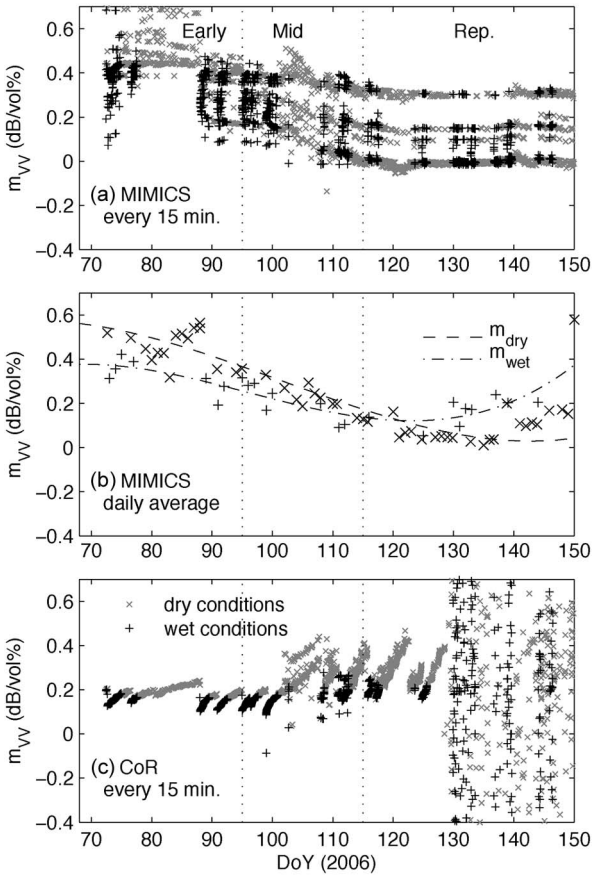

Fig. 3. Sensitivity of $\sigma^0_{\rm terrainVV}$ to changes in SM ($m_{\rm VV} = \Delta\sigma^0_{\rm terrain}/\Delta$SM) at VV pol estimated by: (a) the MIMICS model every 15 min, (b) the MIMICS model daily average, and (c) the CoR model every 15 min. The curve fit for the daily averaged sensitivities in MIMICS are represented by $m_{\rm dry} = 1.95 \times 10^{-6}t^3 - 5.94 \times 10^{-4}t^2 + 0.05t - 0.73$ and $m_{\rm wet} = 3.22 \times 10^{-6}t^3 - 9.27 \times 10^{-4}t^2 + 0.08t - 1.92$ where t is DoY.

B. Sensitivity of $\sigma^0_{\rm terrain}$ to Changes in Soil Moisture

We calculate the sensitivity of $\sigma^0_{\rm terrain}$ estimated by the MIMICS and CoR models to changes in observed SM during the MicroWEX-5 for wet (SM $>$12 vol%) and dry (SM $\leq$ 12 vol%) conditions. Table III shows the mean values of the sensitivities of $\sigma^0_{\rm terrain}$ to changes in observed SM ($\Delta\sigma^0_{\rm terrain}/\Delta$SM) estimated by the two models for the entire growing season and for each stage of growth. During the growing season, the CoR estimated similar sensitivities as the MIMICS model at both co-pols. The sensitivity of the models ranged between 0.15–0.28 dB/vol% at both co-pols (see Table III). The ALOS and SMAP missions have a calibration accuracy in $\sigma^0_{\rm terrain}$ of 0.8–1.5 dB [1], [14], indicating the detection of changes in SM of 2–10 vol% for terrain types similar to the sweet corn.

During the early stage, the $\sigma^0_{\rm terrain}$ in MIMICS exhibited higher sensitivities at VV pol than at HH pol, whereas the CoR model showed similar sensitivities at both co-pols (see Table III). During the mid stage, the $\sigma^0_{\rm terrain}$ in MIMICS exhibited lower sensitivities at VV than at HH pols while CoR showed higher sensitivity at VV than at HH. During the reproductive stage, both the models exhibited lower sensitivities at VV than at HH pol (see Table III). In this study, we focus our discussion to the sensitivities at VV pol during the growing season. Fig. 3(a) and (c) show the sensitivities of $\sigma^0_{\rm terrainVV}$

estimated by the MIMICS and CoR every 15 minutes over the growing season under dry and wet soil conditions mentioned above. Fig. 3(b) shows the daily averages of the sensitivities in the MIMICS model. During the early and mid stages, the $\sigma^0_{\mathrm{terrainVV}}$ estimated by both the models exhibited higher sensitivities during dry conditions, by 0.05–0.27 dB/vol%, than wet conditions [see Fig. 3(b) and (c)]. In contrast, during the reproductive stage, the $\sigma^0_{\mathrm{terrainVV}}$ by the MIMICS model was more sensitive to the SM at wet conditions than at dry conditions [see Fig. 3(b)]. The sensitivities in the CoR model followed similar trends as the SM observations up to DoY 130, when $\sigma^0_{\mathrm{soil}} < -15$ dB. The high sensitivities of CoR at mid stage were because of the high contribution from the $\sigma^0_{\mathrm{se,int}}$ and $\sigma^0_{\mathrm{l,int}}$ [see Fig. 2(c) and (d)]. The CoR model exhibited a high dispersion after DoY 130 due to high contribution from ears. Because the sensitivity of $\sigma^0_{\mathrm{terrainVV}}$ to changes in SM is dependent upon σ^0_{int}, through $\sigma^0_{\mathrm{se,int}}$, during the reproductive stage, the oscillations observed after DoY 130 on $\sigma^0_{\mathrm{se,int}}$ resulted in a high dispersion of $\Delta\sigma^0_{\mathrm{terrainVV}}/\Delta\mathrm{SM}$.

The MIMICS model exhibited the highest sensitivity during the early stage, with detection of SM changes as low as 2 vol%, based upon the ALOS/SMAP calibration accuracy in the $\sigma^0_{\mathrm{terrain}}$ [see Fig. 3(a)]. The CoR model exhibited the highest sensitivity during the mid stage with detection in SM changes as low as 2.5 vol% [see Fig. 3(c)]. However, observations of $\sigma^0_{\mathrm{terrain}}$ at high temporal resolutions are needed to ensure minimal change in vegetation and micrometeorological conditions and further validate these sensitivity values obtained from the model simulations. Such observations will also offer insights into whether the high SM sensitivities in the CoR model, in the presence of significant vegetation, are realistic. The selection of incoherent or coherent approaches also depends upon the knowledge of input parameters and the computing resources available. The incoherent model is computationally simpler and requires less computing resources but calculates amplitudes that are realistic for sweet corn in this study. In contrast, the coherent model is computationally demanding because it utilizes the Monte Carlo method.

VI. Summary and Conclusion

In this study, we compare the backscattering coefficients estimated by the incoherent and coherent approaches at L-band with an incidence angle of 40° for a growing season of sweet corn in Florida using field observations from the MicroWEX-5. The average RMSD between the MIMICS and CoR models over the growing season ranged between 3–4 dB, with higher RMSDs at HH pol, indicating the presence of coherent effects. The $\sigma^0_{\mathrm{se,dir}}$ was the primary contribution in the MIMICS model, whereas the $\sigma^0_{\mathrm{se,int}}$ was the most significant in the CoR model as a result of constructive interferences. The disc-shaped leaves in MIMICS predicted lower $\sigma^0_{\mathrm{l,dir}}$ and $\sigma^0_{\mathrm{l,int}}$ at both pols than those predicted by the ellipsoidal leaves in the CoR model. The MIMICS model exhibited lower sensitivity to dynamic vegetation than the CoR model. Coherent effects were observed in the stem contribution when comparing the estimates by MIMICS and those by CoR, particularly at HH pol. During the early stage, the MIMICS model exhibited the highest sensitivity with a detection in SM changes as low as 2 vol%, based upon the ALOS/SMAP accuracy. During the mid stage, the CoR model exhibited the highest sensitivity with a detection in SM changes as low as 2.5 vol%.

Both the MIMICS and CoR models predicted realistic values of $\sigma^0_{\mathrm{terrain}}$ throughout the growing season. Both the MIMICS model with elliptical leaves and the CoR model with restrictive location of ears could be adequate models to estimate $\sigma^0_{\mathrm{terrain}}$ from a growing corn. However, observations of $\sigma^0_{\mathrm{terrain}}$ at high- temporal resolutions are needed to further validate the model results and to offer insights into whether the high SM sensitivities in the CoR model, in the presence of significant vegetation, are realistic.

Acknowledgment

The authors would like to thank the computational resources and support provided by the University of Florida High-Performance Computing Center for the simulations conducted in this study.

References

[1] A. Rosenqvist, M. Shimada, N. Ito, and M. Watanabe, "ALOS PALSAR: A pathfinder mission for global scale monitoring of the environment," *IEEE Trans. Geosci. Remote Sens.*, vol. 45, no. 11, pp. 3307–3316, Nov. 2007.

[2] Y. Kerr, P. Waldteufel, J. Wigneron, J. Martinuzzi, J. Font, and M. Berger, "Soil moisture retrieval from space: The Soil Moisture and Ocean Salinity (SMOS) mission," *IEEE Trans. Geosci. Remote Sens.*, vol. 39, no. 8, pp. 1729–1735, Aug. 2001.

[3] D. Le Vine, G. Lagerloef, F. Colomb, S. Yueh, and F. Pellerano, "Aquarius: An instrument to monitor sea surface salinity from space," *IEEE Trans. Geosci. Remote Sens.*, vol. 45, no. 7, pp. 2040–2050, Jul. 2007.

[4] D. Entekhabi, E. Njoku, P. O'Neill, M. Spencer, T. Jackson, J. Entin, E. Im, and K. Kellogg, "The Soil Moisture Active/Passive Mission (SMAP)," in *Proc. IEEE IGARSS*, 2008, vol. 3, pp. III-1–III-4.

[5] N. Chauhan, D. Le Vine, and R. Lang, "Discrete scatter model for microwave radar and radiometer response to corn: Comparison of theory and data," *IEEE Trans. Geosci. Remote Sens.*, vol. 32, no. 2, pp. 416–426, Mar. 1994.

[6] J. Stiles, K. Sarabandi, and F. Ulaby, "Electromagnetics scattering from grassland. II. Measurement and modeling results," *IEEE Trans. Geosci. Remote Sens.*, vol. 38, no. 1, pp. 349–356, Jan. 2000.

[7] F. Ulaby, K. Sarabandi, K. McDonald, M. Whitt, and M. Dobson, "Michigan Microwave Canopy Scattering Model (MIMICS)," *Int. J. Remote Sens.*, vol. 11, no. 7, pp. 1123–1153, Jul. 1988.

[8] L. Thirion, I. Chenerie, and C. Galy, "Application of a coherent model in simulating the backscattering coefficient of a mangrove forest," *Waves Random Media*, vol. 14, no. 2, pp. 393–414, Apr. 2004.

[9] J. Casanova, F. Yan, M. Jang, J. Fernandez, J. Judge, C. Slatton, K. Calvin, T. Lin, O. Lanni, and L. W. Miller, Field observations during the Fifth Microwave, Water, and Energy Balance Experiment (MicroWEX-5): From March 9 through May, 2006, Center Remote Sens., Univ. Florida, Gainesville. [Online]. Available: http://edis.ifas.ufl.edu/AE407

[10] M. Zribi and M. Dechambre, "A new empirical model to retrieve soil moisture and roughness from C-band radar data," *Remote Sens. Environ.*, vol. 84, no. 1, pp. 42–52, Jan. 2003.

[11] M. Yang, K. Calvin, J. Casanova, and J. Judge, Measurements of soil surface roughness during the Fourth Microwave Water and Energy Balance Experiment: April 18 through June 13, 2005, Center Remote Sens., Univ. Florida, Gainesville. [Online]. Available: http://edis.ifas.ufl.edu/AE363

[12] N. Peplinski, F. Ulaby, and M. Dobson, "Dielectric properties of soils in the 0.3–1.3 GHz range," *IEEE Trans. Geosci. Remote Sens.*, vol. 33, no. 3, pp. 803–807, May 1995.

[13] F. Ulaby and M. El-Rayes, "Microwave dielectric spectrum of vegetation, Part II: Dual dispersion model," *IEEE Trans. Geosci. Remote Sens.*, vol. GRS-25, no. 5, pp. 550–557, Sep. 1987.

[14] R. West, "SMAP L1 data processing and products," in *Proc. NASA SMAP Algorithm Working Group Meeting*, 2009.

[15] J. Casanova and J. Judge, "Estimation of energy and moisture fluxes for dynamic vegetation using coupled SVAT and crop-growth models," *Water Resour. Res.*, vol. 44, no. 7, pp. 222–241, 2008, W07415, DOI:10.1029/2007WR006503.